Microcirculation
The Official Journal of the Microcirculatory Society, Inc. and the British Microcirculation Society

DOI:10.1111/j.1549-8719.2012.00213.x

Original Article

Cerebral Microcirculatory Responses of Insulin-Resistant Rats are Preserved to Physiological and Pharmacological Stimuli

ADAM INSTITORIS,*,†,[1] LAURA LENTI,*,†,[1] FERENC DOMOKI,† EDINA WAPPLER,‡ TAMÁS GÁSPÁR,† PRASAD V. KATAKAM,*,‡ FERENC BARI,§ AND DAVID W. BUSIJA*,‡

*Department of Physiology and Pharmacology, Wake Forest University Health Sciences, Winston-Salem, North Carolina, USA; †Department of Physiology, School of Medicine, University of Szeged, Szeged, Hungary; ‡Department of Pharmacology, School of Medicine, Tulane University, New Orleans, Louisiana, USA; §Department of Medical Informatics and Medical Physics, School of Medicine, University of Szeged, Szeged, Hungary
Address for correspondence: Adam Institoris, M.D., Ph.D., Department of Physiology, Faculty of Medicine, University of Szeged, Dom ter 10, Szeged H-6720, Hungary. *E-mail:* instiadam@gmail.com

[1]These authors contributed equally to the manuscript.

Received 30 January 2012; accepted 23 July 2012.

ABSTRACT

Objective: Previously, we have shown that IR impairs the vascular reactivity of the major cerebral arteries of ZO rats prior to the occurrence of Type-II diabetes mellitus. However, the functional state of the microcirculation in the cerebral cortex is still being explored.

Methods: We tested the local CoBF responses of 11–13-week-old ZO ($n = 31$) and control ZL ($n = 32$) rats to several stimuli measured by LDF using a closed cranial window setup.

Results: The topical application of 1–100 μM bradykinin elicited the same degree of CoBF elevation in both ZL and ZO groups. There was no significant difference in the incidence, latency, and amplitude of the NMDA-induced CSD-related hyperemia between the ZO and ZL groups. Hypercapnic CoBF response to 5% carbon-dioxide ventilation did not significantly change in the ZO compared with the ZL. Topical bicuculline-induced cortical seizure was accompanied by the same increase of CoBF in both the ZO and ZL at all bicuculline doses.

Conclusions: CoBF responses of the microcirculation are preserved in the early period of the metabolic syndrome, which creates an opportunity for intervention to prevent and restore the function of the major cerebral vascular beds.

Key words: Zucker obese, cortical spreading depression, *N*-methyl-D-aspartate, bicuculline, hypercapnia

Abbreviations used: aCSF, artificial cerebrospinal fluid; ANOVA, analysis of variance; CoBF, cortical blood flow; COX-1, cyclooxygenase-1; CSD, cortical spreading depression; DC, direct current; EEG, electroencephalogram; eNOS, endothelial nitric oxide synthase; GABA, gamma-aminobutyric acid; i.p., intraperitoneal; IR, insulin resistance; K_{Ca}, Ca^{2+}-dependent K^+; K_{ATP}, ATP-sensitive K^+; LDF, laser Doppler flowmetry; L-NAME, L-nitro-arginine methyl ester; MABP, mean arterial blood pressure; NMDA, *N*-methyl-D-aspartate; NO, nitric oxide; ROS, reactive oxygen species; SEM, standard error of the mean; ZL, Zucker lean; ZO, Zucker obese.

Please cite this paper as: Institoris A, Lenti L, Domoki F, Wappler E, Gáspár T, Katakam PV, Bari F, Busija DW. Cerebral microcirculatory responses of insulin-resistant rats are preserved to physiological and pharmacological stimuli. *Microcirculation* **19**: 749–756, 2012.

INTRODUCTION

IR is a hallmark feature of the metabolic syndrome that is one of the most serious risk factors for cardiovascular and cerebrovascular diseases affecting 24 million people in the United States [10]. Several clinical studies have reported increased prevalence of acute myocardial infarction and ischemic stroke in patients with metabolic syndrome and Type-II diabetes [26,44,56,57]. IR is known to initiate detrimental changes in many vascular beds well before plasma glucose levels increase into the range to meet the diagnostic criteria of Type-II diabetes. Thus, appropriate animal models need to be used to mimic this important stage of the metabolic syndrome. In rats, IR can be induced with fructose feeding [15,34], but a more widely used and accepted model of metabolic syndrome is the homozygous leptin receptor-deficient ZO rat. At the age of 11–13 weeks, these ZO animals are "pre-diabetic," characterized by IR,

elevated plasma cholesterol, and triglyceride levels, but with normal blood pressure and glucose levels as shown previously in our laboratory [17]. The ZL strain, which is heterozygous for the mutation, has normal physiological parameters and can be used as a control group.

Using these animal models, numerous biochemical and molecular changes in the vasculature were shown to be associated with IR. Vascular dysfunction of coronary arteries [33], mesenteric arteries [59], skeletal muscle arteries [28], and major cerebral arteries [9] has all been described previously. The quantitative measurement of multiple organ blood flow showed that several tissues (adiposal tissue, intestine, and kidney) had a reduced blood flow in a special type of ZO strain, the Zucker diabetic fatty rats, whereas baseline cerebral perfusion remained normal even at a progressive diabetic stage [54]. Stepp *et al.* measured internal carotid blood flow with ultrasonic flowmetry in 13–15-week-old ZO and ZL rats and found similar blood flow values [55]. However, earlier works from our laboratory have described abnormal vascular functioning focusing mainly on the large arteries of the cerebral vasculature. Major cerebral arteries of ZO/fructose-fed rats in the pre-diabetic period showed reduced endothelium-dependent and -independent relaxations to various stimuli under both *in vivo* and *ex vivo* conditions [13–15,17]. In contrast, the constrictor responses of the basilar artery were found to be either unaffected or augmented in these animals [16]. The abnormal reactivity of main cerebral vessels is worsened in the 17-week-old diabetic ZO rat [48]. The observed vascular dysfunction of the cerebral arteries probably contributes to the higher vulnerability of ZO animals to both ischemic [46] and hemorrhagic stroke [32]. Despite the thorough investigation of IR-induced dysfunction of the major cerebral arteries, little is known about the effect of IR on microvascular reactivity at the level of the local cortical microcirculation in both pre-diabetic and diabetic stages. Interestingly, the endothelium-independent CSD-induced hyperemia was found to be unaltered in fructose-fed diabetic rats, indicating that cerebrovascular dysfunction may be limited to specific vasodilatory mechanisms [52]. As baseline cerebral blood flow is preserved in IR but the reactivity of major cerebral arteries is impaired when stimulated, in the present study, we examined local cortical microvascular reactivity to various physiological and pharmacological stimuli, which increase cortical perfusion via multiple, independent signaling pathways to detect early microvascular dysfunction in IR using ZO rats. We also entertained the possibility that restricted dilation of larger arteries might not interfere with total CoBF responses to dilator stimuli. In an earlier study in dogs, we found that fixation of surface arteries at a constant diameter with cyanoacrylate glue did not reduce resting CoBF or CoBF responses to arterial hypercapnia measured with radioactive microspheres [8].

Therefore, we tested the effect of the following: (1) bradykinin, (2) NMDA, (3) hypercapnia (5% CO_2), and (4) bicuculline ($GABA_A$-type receptor blocker) on CoBF changes measured with LDF. Bradykinin and hypercapnia have direct effects on cerebral resistance blood vessels, whereas NMDA and bicuculline have vascular effects secondary to neuronal activity (NMDA directly increases neuronal activity, whereas bicuculline indirectly increases neuronal activity by removing inhibitory influences). LDF has been shown to be a valid indicator of changes in CoBF, but as with all methods used to characterize cerebral vascular responses, it has some limitations that need to be considered in the interpretation of the results.

MATERIALS AND METHODS

Surgery

Male ZL (n = 32, 11–12 weeks old, body weight=346±42g) and ZO (n = 31, 11–12 weeks old, body weight=536±43g) rats were used for the experiments. Animals were maintained and used in compliance with the principles set forth by the Animal Care and Use Committee of Wake Forest University Health Sciences. The surgery and cranial window preparation were carried out as described previously [37]. In a previous unpublished study with *ad libitum* overnight food access, the blood sugar level for ZO rats (n = 11; body weight = 516 ± 35 g) was 179 ± 48 mg/dL and for ZL rats (n = 10; body weight = 321 ± 28), it was 124 ± 57 mg/dL (mean ± SD). For rats with six hours of fasting, the average blood sugar level for ZO was 121 ± 31 mg/dL, and for ZL rats, it was 115 ± 32 mg/dL (mean + SD). Glycated hemoglobin (HbA1C) levels were 4.5 ± 0.3% in ZL and 5.3 ± 0.5% in ZO animals (A1CNow+®, Bayer, Sunnyvale, CA, USA). Anesthesia was induced with i.p. administration of pentobarbital (80 mg/kg) and maintained by an infusion pump (20 mg/kg/h) via a catheter introduced into the femoral vein. The rats were mechanically ventilated with room air supplemented with O_2. The end-tidal CO_2 level was continuously monitored with a capnograph (Micro-Capnometer; Columbus Instruments, Columbus, OH, USA) and ventilation was adjusted to maintain 40 mmHg end-tidal CO_2 tension. A catheter was introduced into the femoral artery to obtain blood samples for blood gas measurements (see Results) and to monitor and keep the MABP within the physiological range (ZL rats = 84 ± 5 mmHg; ZO rats = 95±4 mmHg; mean ± SEM). Body temperature was monitored by a rectal probe and maintained at 37°C by a water-circulating heating pad. The head of the animal was fixed in a stereotaxic frame, the skin of the scalp was retracted, and a 4-mm diameter circular craniotomy was prepared on the right parietal bone. The brain surface was continuously moisturized with aCSF (composition in mg/L: 220 KCl, 7714 NaCl, 665 dextrose, 251.4 $CaCl_2$, 61.9 $MgCl_2$,

and 2066.6 $NaHCO_3$). The dura mater was carefully dissected and a circular 2-mm high bone wax rim was mounted around the craniotomy, which was strengthened with cyanoacrylate. Inflow and outflow ports were inserted into the rim to enable flushing of the brain and administration of drugs onto the brain surface. To verify the DC potential shift during CSD, an Ag/AgCl electrode was positioned over the dura mater through a burr hole 2 mm rostral to the cranial window. In animals where EEG was measured instead of DC potential to prove bicucculine-induced seizure activity, a second Ag/AgCl electrode was placed onto the cortical surface under the cranial window through the outflow port. The ground lead was inserted under the skin of the neck. The electrodes were connected to an AC–DC amplifier (DAM 50, differential amplifier; World Precision Instruments, Sarasota, FL, USA) for the recording of DC potential changes or EEG signals (AC mode, 100 Hz filter), respectively. A laser Doppler probe (Periflux 4001 master; Perimed, Stockholm, Sweden) was placed above the parietal cortex (lambda 3 mm, bregma −4 mm) to measure CoBF. The window was closed with a Parafilm® foil and filled with aCSF. In those animals in which we expected CSD appearance and propagation following NMDA application, a second laser Doppler probe was placed 8 ± 1 mm rostral to the first one. CoBF, DC potential or EEG, MABP, and end-tidal CO_2 were continuously recorded and stored on a personal computer with the IOX software (EMKA Technologies, Falls Church, VA, USA). After filling and washing the window with aCSF and also before each stimulus, we recorded eight minutes CoBF baseline. At the end of the experiments, biological zero of the laser-Doppler signal was measured following over-anesthesia and i.v. saturated KCl injection.

Data Analysis

The biological zero values were subtracted from the recorded data, were averaged for every minute, and were normalized to the respective averaged baseline values. The CoBF data were then expressed as the percentage change from baseline and the maximal CoBF response occurring over a one-minute interval was determined. When CSDs occurred (during NMDA applications), the maximal increase in the CoBF response (peak), the delay or latency from the beginning of drug application to the peak CoBF, and the post-CSD hyperemic wave were determined by calculating the average CoBF change in the 60–360th seconds after the peak. The dose-dependent effects of the different stimulations were statistically compared between the ZO and ZL groups with two-way measures ANOVA or two-way repeated measures ANOVA, accordingly, followed by the Tukey *post-hoc* test (Sigmastat 3.5; Systat Software Inc., San Jose, CA, USA). To compare the incidence of CSD triggered by NMDA, we performed the *z*-test.

Experimental Protocol

Before each topical stimulation, aCSF was superfused over the window using the same rate (1 mL/min) as the consecutive drug application to make sure that washing of the window did not change baseline flow. We did not find any change in the laser-Doppler signal in any of the rats tested during control aCSF superfusion (data not shown). The first set of ZL ($n = 9$) and ZO ($n = 9$) animals were stimulated with increasing doses of bradykinin (1–100 μM; Sigma–Aldrich, St. Louis, MO, USA) topically on the brain surface. After five minutes of baseline recording, the topical application took four minutes, after which the window was washed with 1 mL aCSF over a one-minute period. Then, the next baseline was recorded. On the second set of ZL ($n = 9$) and ZO ($n = 9$) animals, increasing doses (10^{-5}–10^{-3} M) of NMDA (Sigma–Aldrich) were administered onto the brain surface for 10 minutes each.

In the third experimental group, following baseline recording, 14 ZL and 13 ZO rats were ventilated with 5% CO_2 for five minutes. After hypercapnia, ventilation was switched back to room air. After 20 minutes, the cranial windows were superfused with 10^{-4} M, then with 5×10^{-4}, and finally with 10^{-3} M bicucilline-methiodide (Tocris Bioscience, St. Louis, MO, USA), for 10 minutes for each dose. The window was then washed every 10 minutes with aCSF for one hour.

RESULTS

The topical application of bradykinin (Figure 1) dose-dependently increased the CoBF in both the ZL and ZO animals with 9 ± 2% and 11 ± 4% (1 μM), 21 ± 4% and 27 ± 6% (10 μM), and 42 ± 12% and 42 ± 10% (100 μM),

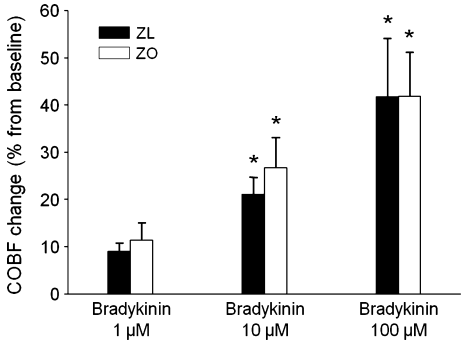

Figure 1. The effect of increasing doses of topical bradykinin (1, 10, and 100 μM) on CoBF change from baseline in ZL (black columns) and ZO (white columns) rats. Data presented are the average of the 10th minute of bradykinin application. Data are mean ± SEM; ($n = 7$–7; $*p < 0.05$; 1 μM vs. 10 μM and 1 μM vs. 100 μM).

respectively. No significant difference was detected between the two groups at any dose.

Although NMDA induced marked increases in CoBF, these perfusion changes were confounded by NMDA-induced CSDs. Thus, the typical response for topical NMDA application consisted of a CSD-related, fast and large hyperemic response followed by a milder, but more sustained, CoBF increase (Figure 2A and B). We identified a CoBF response to NMDA as CSD-induced if it was accompanied by a negative DC-potential shift and a similar CoBF response was recorded after appropriate delay under the second, frontal laser Doppler probe outside the cranial window during the stimulation period (10 minutes). Six of nine rats had CSD responses in both the ZL and the ZO groups for the lower (10^{-4} M) dose of NMDA, while all ZL and ZO rats (9/9) showed CSD with the 10^{-3} M dose of NMDA. To compare the responses of the different NMDA doses, only animals in which CSD was evoked by both NMDA doses ($n = 6$–6) were included in the statistical analysis. The latency of CSD peak appearance (Figure 2C) was significantly shorter for the higher vs. the lower dose of NMDA in both groups ($p < 0.05$), but was not different in the ZO group both at 10^{-4} M (158 ± 8 s) and at 10^{-3} M (118 ± 4 s) NMDA from the ZL (177 ± 15 and 122 ± 13 s) counterpart. The peak amplitude during the CSD response (Figure 2D) was higher in response to the 10^{-3} M NMDA (ZL = 176 ± 34%; ZO = 242 ± 21%) in comparison with the 10^{-4} M NMDA (ZL = 110 ± 29%; ZO = 182 ± 12%; $p < 0.01$), but again, no significant difference was found at any dose between the ZO and ZL groups ($p > 0.08$). Although the magnitude of the post-CSD hyperemia (Figure 2E) was significantly higher by 10^{-3} M NMDA (ZL = 75 ± 18%; ZO = 60 ± 11%) than by the 10^{-4} M NMDA, the degree of flow increase (ZL = 23 ± 12%; ZO = 19 ± 8%; $p < 0.05$) in both the ZL and ZO rats was similar.

Ventilation with 5% CO_2 for five minutes caused mild (ZL: pH = 7.28 ± 0.01, pCO_2 = 47 ± 4 mmHg; ZO: pH =7.31 ±0.02, pCO_2 = 46 ± 4 mmHg) hypercapnia in both groups compared with baseline blood gas values (ZL: pH=7.42 ± 0.01, pCO_2 = 36 ± 3 mmHg; ZO: pH = 7.42 ± 0.02, pCO_2 = 36 ± 1 mmHg; mean ± SD), which were similar in the ZL and the ZO rats. During hypercapnia, the CoBF increase to 5% CO_2 ventilation (Figure 3) after five minutes was 20 ± 4% in the ZL and 22 ± 3% in the ZO. Thus, we did not find any statistical difference between the ZL and ZO groups.

Bicuculline administration onto the brain surface resulted in cortical seizure activity detected by EEG (Figure 4A), which was coupled with a time- and dose-dependent rise in CoBF (Figure 4B), showing 30 ± 10% in ZL and 36 ± 15% in ZO rats at 10^{-4} M dose, 66 ± 11% in the ZL and 68 ± 18% in the ZO at 5×10^{-4} M dose, and 95 ± 12% for the ZL vs. 88 ± 19% in the ZO group by the 10th minute of drug administration ($p < 0.05$). Similarly, the values of the ZL and ZO groups were not statistically different.

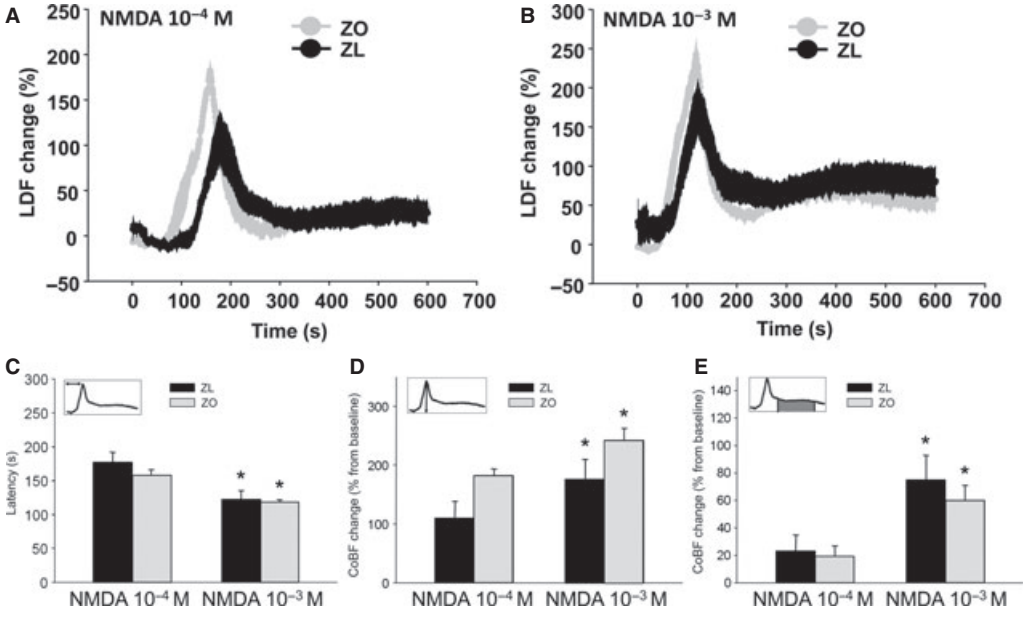

Figure 2. The CoBF response curves to 10^{-4} M NMDA (**A**) and to 10^{-3} M NMDA (**B**) in ZO ($n = 5$; gray curves) and ZL ($n = 6$) rats (black curves) represented by LDF changes. (**C**) The latency to CoBF-peak was expressed in seconds, (**D**) peak amplitude, and (**E**) the average of post-peak sustained hyperemia (from one minute post-peak for five minutes) following NMDA application were expressed as percentage increase from a five-minute baseline period. Black column: ZL; white column: ZO. The CoBF data are presented as mean ± SEM and analyzed with two-way repeated measures analysis of variance ($n = 5$–6, *$p < 0.05$ for NMDA 10^{-4} M dose vs. NMDA 10^{-3} M dose).

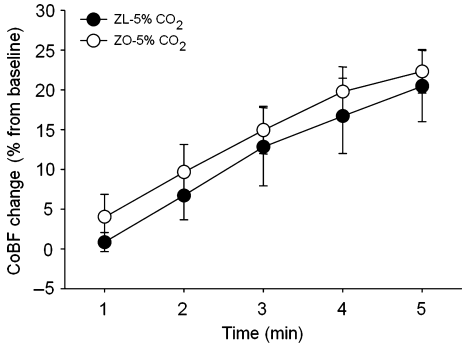

Figure 3. Temporal changes of CoBF during five minutes of 5% CO_2 ventilation (n = 12–14) in ZO (white column) and ZL (black column) rats. The CoBF data are presented as mean ± SEM and analyzed with two-way repeated measures analysis of variance.

DISCUSSION

The most important finding of our study is that microvascular reactivity of the cerebrocortical microcirculation is intact after exposure to multiple complex stimuli in IR but not yet diabetic ZO rats. The assessed vascular stimuli consisted of mild physiologic changes (such as CO_2 sensitivity; Figure 3) and more severe challenges (CSD, seizures; Figures 2 and 4) in which the appropriate reaction of the microvasculature is crucial to prevent cortical tissue injury. Therefore, in contrast to the large cerebral arteries, the responses of the microcirculatory system in the brain are intact during the early phase of IR.

In this study, we first examined the vasoactive effect of bradykinin, a peptide mediating inflammation-related hyperemia [39,43]. Bradykinin is produced in high amounts during brain injury and inflammation. It directly dilates major cerebral [14] and pial arterioles [6] and also indirectly by releasing vasoactive glutamate from astrocytes [39]. The mechanism of bradykinin-mediated dilation in cerebral arterioles involves endothelial NO produced by eNOS and COX-1-produced ROS [6,45,51,53,61], which activate K_{Ca} channels on the surface of smooth muscle cells [53]. Previously, we found that dilation of the middle cerebral artery to bradykinin is reduced in fructose-fed IR rats [14]. In contrast, our current data (Figure 1) show that the dilation of arterioles to bradykinin is preserved in ZO rats, suggesting that dilatory pathways, which involve eNOS, COX-1, ROS, and K_{Ca} channel, are not functionally impaired or that different compensatory pathways are activated at the level of microcirculation in IR.

Our second purpose was to explore the characteristics of NMDA-induced CoBF changes. NMDA is a potent *in vivo* dilator of cerebrocortical microvessels through a unique neuro-vascular mechanism [7]. More recently, NMDA has been shown to generate CSD in the mouse [2]. We recently showed that NMDA-induced cortical hyperemia is induced by CSD-dependent and -independent mechanisms in the rat cortex [37]. CSD is a wave of depolarization, which propagates over the cortical surface accompanied by a sudden increase in tissue perfusion. It is associated with migraine attacks, and it exaggerates stroke following ischemic and/or hemorrhagic stroke [12,23,36]. In this study, NMDA application onto the brain surface of ZO and ZL rats produced a dose-dependent CoBF elevation, starting with a CSD-related peak hyperemia followed by a prolonged hyperemic phase (Figure 2), which is in accordance with our previous finding in Wistar rats [37]. The mechanism of NMDA-mediated CoBF response involves multiple cells and signaling pathways [7,50]. In the rat cortex, the CSD-induced cerebrovascular response is resistant to the non-selective NOS blocker, L-NAME [20,52]. On the other hand, the NMDA-induced-, presumably CSD-independent, cortical vasodilation [3,22] and hyperemic [60] response were abolished by the selective neuronal NOS inhibitor 7-nitroindazole. NMDA-induced neuronal NO release and vasodilation seem to be an astroglia and endothelium-independent process [4,11,21], and it presumably activates K_{ATP} channels and K_{Ca} channels on the vascular smooth muscle surface [47]. Our earlier experiments on the basilar artery *in vivo* and on the isolated middle cerebral artery clearly showed that K_{Ca}- and K_{ATP}-channel-mediated dilations are significantly reduced in fructose-fed IR rats as well as in ZO rats [15,17,18,32]. Importantly, these vascular dysfunctions were reversed with antioxidant enzymes [15,17] and protein kinase C antagonists [17]. This study shows that neither the CSD-related, nor the sustained post-CSD hyperemia deteriorated in the cortex of IR rats.

Third, we studied the effect of topical bicuculline application on CoBF (Figure 4). Our findings confirm that bicuculline elevates tissue perfusion [40] as a surrogate of increased neuronal firing rate [41]. The seizure-induced CoBF response is complex and is related to the compound effects of local tissue acidosis [29,38], elevated extracellular K^+ [24,35], and adenosine levels [5] released from astrocytes and activated neurons [1,42]. The dilation of the basilar artery to high extracellular K^+ levels was shown to be reduced in IR [17]. The similar dose-dependent CoBF response of ZO and ZL strains to bicuculline in addition to NMDA further confirms the hypothesis that neuronal activity-coupled hemodynamic responses are indeed preserved in IR.

To our knowledge, our study is the first to investigate the CO_2 response of the cerebral circulation in IR. We found that the CO_2 response to 5% CO_2 of IR rats remained unchanged (Figure 3), which suggests simultaneous intact reactivity of the microvasculature. Hypercapnic hyperemia is induced by extraluminal acidosis and is mediated by NO [19,30,31], prostaglandins [27], and adenosine [19,49], factors which relax the smooth muscle cells via K_{Ca} and K_{ATP} channels [38]. Previous studies have shown that cerebral vascular

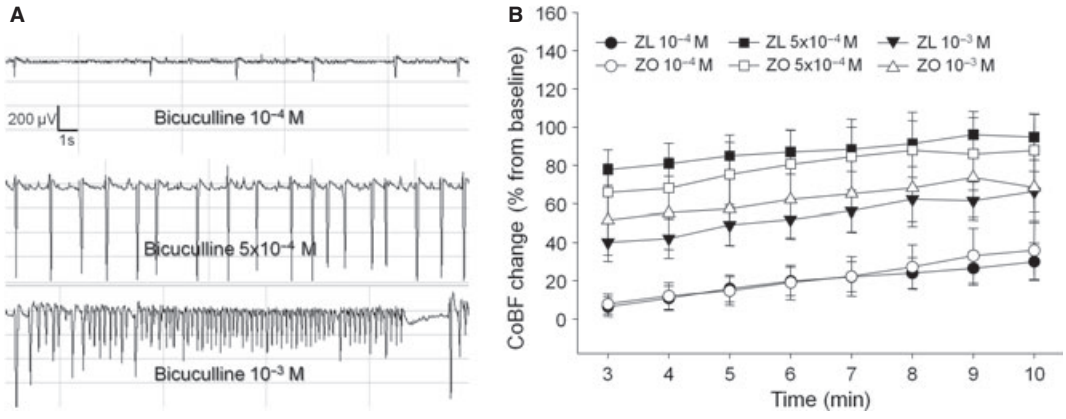

Figure 4. (**A**) Representative EEG recorded during the incubation with 10^{-4}, 5×10^{-4}, and 10^{-3} M topical bicuculline, and (**B**) CoBF changes from the 3rd to the 10th minute of bicuculline applications (n = 12–11) in ZO (white column) and ZL (black column) rats. The CoBF data are presented as mean ± SEM and analyzed with two-way repeated measures analysis of variance.

dilation to hypercapnia occurs primarily in the small cerebral arteries, while dilation of larger arteries is restricted by activation of sympathetic nerves [58]. Our finding is in concert with human studies where the cerebrovascular reactivity after acetazolamide stimulation (inducing local hypercapnia and acidosis) was reduced in long-term (>10 years) diabetic patients, but not in short-term (<10 years) diabetic patients [25].

LDF has several advantages over other methods for characterizing cerebral hemodynamics including ease of application, the ability to continuously monitor CoBF during changing conditions in the same animal, and a history of extensive use and validation under a variety of experimental conditions. Nonetheless, potential drawbacks are that absolute CoBF values cannot be determined and that the LDF might not be sensitive enough to detect differences in CoBF responses between ZO and ZL animals because of the limited depth of penetration of the laser light and because of the restricted area of the cortex that is examined by the probe. On the other hand, other *in vivo* methods for measuring CoBF also have serious drawbacks that make the interpretation of results difficult. For example, the microsphere method necessitates the permanent occlusion of one carotid artery for placement of the intracardiac catheter for injection of the microspheres, which restricts increases in blood flow to both cortices. Similarly, the use of diffusible tracers such as C^{14} iodoantipyrine is technically difficult because of repeated withdrawal of significant amounts of blood, and allows only one CoBF measurement in each animal so that repeated determinations are not possible in each animal. Thus, we are cautious in our conclusions until the results can be validated with another, independent approach, such as multi-photon microscopy. Furthermore, we cannot assert that CoBF responses to other stimuli or conditions would be similarly unaffected by IR.

PERSPECTIVE

In summary, on the basis of our findings, we suggest that the deleterious effect of IR in the pre-diabetic stage is limited to the major cerebral vessels, and that the local control of cerebrocortical microcirculation is preserved in response to the robust stimuli employed in our study. These findings replicate earlier findings in dogs in which fixation of the surface arteries by cyanoacrylate glue did not reduce increases in CoBF to hypercapnia [8]. Previous studies showed reversible dysfunction of major cerebral arteries at this level of IR in the same animal model.

ACKNOWLEDGMENTS

We thank Nancy Busija for editing the manuscript. This work was supported by National Heart, Lung, and Blood Institute Grants HL-030260, HL-065380, HL-077731, and HL-093554, Hungarian Scientific Research Fund Grant OTKA K81266, and TÁMOP-4.2.1./B-09/1/konv-2010–0005. Ferenc Domoki was supported by the János Bolyai Research Scholarship of the Hungarian Academy of Sciences.

REFERENCES

1. Attwell D, Buchan AM, Charpak S, Lauritzen M, Macvicar BA, Newman EA. Glial and neuronal control of brain blood flow. *Nature* 468: 232–243, 2010.
2. Ayata C, Moskowitz MA. Cortical spreading depression confounds concentration-dependent pial arteriolar dilation during *N*-methyl-D-aspartate superfusion. *Am J Physiol Heart Circ Physiol* 290: H1837–H1841, 2006.
3. Bari F, Errico RA, Louis TM, Busija DW. Differential effects of short-term hypoxia and hypercapnia on *N*-methyl-D-aspartate-induced cerebral vasodilatation in piglets. *Stroke* 27: 1634–1639, 1996; discussion 1639–1640.

4. Bari F, Thore CR, Louis TM, Busija DW. Inhibitory effects of hypoxia and adenosine on *N*-methyl-D-aspartate-induced pial arteriolar dilation in piglets. *Brain Res* 780: 237–244, 1998.
5. Boison D. Adenosine and epilepsy: from therapeutic rationale to new therapeutic strategies. *Neuroscientist* 11: 25–36, 2005.
6. Brian JE Jr., Faraci FM, Moore SA. COX-2-dependent delayed dilatation of cerebral arterioles in response to bradykinin. *Am J Physiol Heart Circ Physiol* 280: H2023–H2029, 2001.
7. Busija DW, Bari F, Domoki F, Louis T. Mechanisms involved in the cerebrovascular dilator effects of *N*-methyl-D-aspartate in cerebral cortex. *Brain Res Rev* 56: 89–100, 2007.
8. Busija DW, Heistad DD, Marcus ML. Continuous measurement of cerebral blood flow in anesthetized cats and dogs. *Am J Physiol* 241: H228–H234, 1981.
9. Busija DW, Miller AW, Katakam P, Simandle S, Erdos B. Mechanisms of vascular dysfunctionin insulin resistance. *Curr Opin Investig Drugs* 5: 929–935, 2004.
10. Church T. Exercise in obesity, metabolic syndrome, and diabetes. *Prog Cardiovasc Dis* 53: 412–418, 2011.
11. Domoki F, Perciaccante JV, Shimizu K, Puskar M, Busija DW, Bari F. *N*-methyl-D-aspartate-induced vasodilation is mediated by endothelium-independent nitric oxide release in piglets. *Am J Physiol Heart Circ Physiol* 282: H1404–H1409, 2002.
12. Dreier JP. The role of spreading depression, spreading depolarization and spreading ischemia in neurological disease. *Nat Med* 17: 439–447, 2011.
13. Erdos B, Miller AW, Busija DW. Alterations in KATP and KCa channel function in cerebral arteries of insulin-resistant rats. *Am J Physiol Heart Circ Physiol* 283: H2472–H2477, 2002a.
14. Erdos B, Miller AW, Busija DW. Impaired endothelium-mediated relaxation in isolated cerebral arteries from insulin-resistant rats. *Am J Physiol Heart Circ Physiol* 282: H2060–H2065, 2002b.
15. Erdos B, Simandle SA, Snipes JA, Miller AW, Busija DW. Potassium channel dysfunction in cerebral arteries of insulin-resistant rats is mediated by reactive oxygen species. *Stroke* 35: 964–969, 2004a.
16. Erdos B, Snipes JA, Kis B, Miller AW, Busija DW. Vasoconstrictor mechanisms in the cerebral circulation are unaffected by insulin resistance. *Am J Physiol Regul Integr Comp Physiol* 287: R1456–R1461, 2004b.
17. Erdos B, Snipes JA, Miller AW, Busija DW. Cerebrovascular dysfunction in Zucker obese rats is mediated by oxidative stress and protein kinase C. *Diabetes* 53: 1352–1359, 2004c.
18. Erdos B, Snipes JA, Tulbert CD, Katakam P, Miller AW, Busija DW. Rosuvastatin improves cerebrovascular function in Zucker obese rats by inhibiting NAD(P)H oxidase-dependent superoxide production. *Am J Physiol Heart Circ Physiol* 290: H1264–H1270, 2006.
19. Estevez AY, Phillis JW. Hypercapnia-induced increases in cerebral blood flow: roles of adenosine, nitric oxide and cortical arousal. *Brain Res* 758: 1–8, 1997.
20. Fabricius M, Akgoren N, Lauritzen M. Arginine-nitric oxide pathway and cerebrovascular regulation in cortical spreading depression. *Am J Physiol* 269: H23–H29, 1995.
21. Faraci FM, Breese KR. Nitric oxide mediates vasodilatation in response to activation of *N*-methyl-D-aspartate receptors in brain. *Circ Res* 72: 476–480, 1993.
22. Faraci FM, Brian JE Jr., Heistad DD. Response of cerebral blood vessels to an endogenous inhibitor of nitric oxide synthase. *Am J Physiol* 269: H1522–H1527, 1995.
23. Farkas E, Pratt R, Sengpiel F, Obrenovitch TP. Direct, live imaging of cortical spreading depression and anoxic depolarisation using a fluorescent, voltage-sensitive dye. *J Cereb Blood Flow Metab* 28: 251–262, 2008.
24. Filosa JA, Bonev AD, Straub SV, Meredith AL, Wilkerson MK, Aldrich RW, Nelson MT. Local potassium signaling couples neuronal activity to vasodilation in the brain. *Nat Neurosci* 9: 1397–1403, 2006.
25. Fulesdi B, Limburg M, Molnar C, Kaplar M, Bereczki D, Neuwirth G, Csiba L. [Cerebrovascular reactivity in non-insulin dependent diabetes mellitus (preliminary results)]. *Orv Hetil* 139: 1789–1792, 1998.
26. Haratz S, Tanne D. Diabetes, hyperglycemia and the management of cerebrovascular disease. *Curr Opin Neurol* 24: 81–88, 2010.
27. Heinert G, Nye PC, Paterson DJ. Nitric oxide and prostaglandin pathways interact in the regulation of hypercapnic cerebral vasodilatation. *Acta Physiol Scand* 166: 183–193, 1999.
28. Hodnett BL, Xiang L, Dearman JA, Carter CB, Hester RL. K(ATP)-mediated vasodilation is impaired in obese Zucker rats. *Microcirculation* 15: 485–494, 2008.
29. Horiuchi T, Dietrich HH, Hongo K, Goto T, Dacey RG Jr. Role of endothelial nitric oxide and smooth muscle potassium channels in cerebral arteriolar dilation in response to acidosis. *Stroke* 33: 844–849, 2002.
30. Iadecola C, Zhang F. Permissive and obligatory roles of NO in cerebrovascular responses to hypercapnia and acetylcholine. *Am J Physiol* 271: R990–R1001, 1996.
31. Iadecola C, Zhang F, Xu X. SIN-1 reverses attenuation of hypercapnic cerebrovasodilation by nitric oxide synthase inhibitors. *Am J Physiol* 267: R228–R235, 1994.
32. Institoris A, Snipes JA, Katakam PV, Domoki F, Boda K, Bari F, Busija DW. Impaired vascular responses of insulin-resistant rats after mild subarachnoid hemorrhage. *Am J Physiol Heart Circ Physiol* 300: H2080–H2087, 2011.
33. Katakam PV, Tulbert CD, Snipes JA, Erdos B, Miller AW, Busija DW. Impaired insulin-induced vasodilation in small coronary arteries of Zucker obese rats is mediated by reactive oxygen species. *Am J Physiol Heart Circ Physiol* 288: H854–H860, 2005.
34. Katakam PV, Ujhelyi MR, Hoenig ME, Miller AW. Endothelial dysfunction precedes hypertension in diet-induced insulin resistance. *Am J Physiol* 275: R788–R792, 1998.
35. Knot HJ, Zimmermann PA, Nelson MT. Extracellular K(+)-induced hyperpolarizations and dilatations of rat coronary and cerebral arteries involve inward rectifier K(+) channels. *J Physiol* 492: 419–430, 1996.
36. Lauritzen M, Dreier JP, Fabricius M, Hartings JA, Graf R, Strong AJ. Clinical relevance of cortical spreading depression in neurological disorders: migraine, malignant stroke, subarachnoid and intracranial hemorrhage, and traumatic brain injury. *J Cereb Blood Flow Metab* 31: 17–35, 2010.
37. Lenti L, Domoki F, Gaspar T, Snipes JA, Bari F, Busija DW. *N*-methyl-D-aspartate induces cortical hyperemia through cortical spreading depression-dependent and -independent mechanisms in rats. *Microcirculation* 16: 629–639, 2009.
38. Lindauer U, Vogt J, Schuh-Hofer S, Dreier JP, Dirnagl U. Cerebrovascular vasodilation to extraluminal acidosis occurs via combined activation of ATP-sensitive and Ca^{2+}-activated potassium channels. *J Cereb Blood Flow Metab* 23: 1227–1238, 2003.
39. Liu HT, Akita T, Shimizu T, Sabirov RZ, Okada Y. Bradykinin-induced astrocyte-neuron signalling: glutamate release is mediated by ROS-activated volume-sensitive outwardly rectifying anion channels. *J Physiol* 587: 2197–2209, 2009.
40. Ma H, Zhao M, Suh M, Schwartz TH. Hemodynamic surrogates for excitatory membrane potential change during interictal epileptiform events in rat neocortex. *J Neurophysiol* 101: 2550–2562, 2009.
41. Ma HT, Wu CH, Wu JY. Initiation of spontaneous epileptiform events in the rat neocortex in vivo. *J Neurophysiol* 91: 934–945, 2004.
42. Magistretti PJ, Pellerin L. Astrocytes couple synaptic activity to glucose utilization in the brain. *News Physiol Sci* 14: 177–182, 1999.

43. Moskowitz MA. Basic mechanisms in vascular headache. *Neurol Clin* 8: 801–815, 1990.
44. Najarian RM, Sullivan LM, Kannel WB, Wilson PW, D'Agostino RB, Wolf PA. Metabolic syndrome compared with type 2 diabetes mellitus as a risk factor for stroke: the Framingham Offspring Study. *Arch Intern Med* 166: 106–111, 2006.
45. Niwa K, Haensel C, Ross ME, Iadecola C. Cyclooxygenase-1 participates in selected vasodilator responses of the cerebral circulation. *Circ Res* 88: 600–608, 2001.
46. Osmond JM, Mintz JD, Dalton B, Stepp DW. Obesity increases blood pressure, cerebral vascular remodeling, and severity of stroke in the Zucker rat. *Hypertension* 53: 381–386, 2009.
47. Philip S, Armstead WM. NMDA dilates pial arteries by KATP and Kca channel activation. *Brain Res Bull* 63: 127–131, 2004.
48. Phillips SA, Sylvester FA, Frisbee JC. Oxidant stress and constrictor reactivity impair cerebral artery dilation in obese Zucker rats. *Am J Physiol Regul Integr Comp Physiol* 288: R522–R530, 2005.
49. Phillis JW, Lungu CL, Barbu DE, O'Regan MH. Adenosine's role in hypercapnia-evoked cerebral vasodilation in the rat. *Neurosci Lett* 365: 6–9, 2004.
50. Reuter U, Weber JR, Gold L, Arnold G, Wolf T, Dreier J, Lindauer U, Dirnagl U. Perivascular nerves contribute to cortical spreading depression-associated hyperemia in rats. *Am J Physiol* 274: H1979–H1987, 1998.
51. Rosenblum WI. Hydroxyl radical mediates the endothelium-dependent relaxation produced by bradykinin in mouse cerebral arterioles. *Circ Res* 61: 601–603, 1987.
52. Shimizu K, Miller AW, Erdos B, Bari F, Busija DW. Role of endothelium in hyperemia during cortical spreading depression (CSD) in the rat. *Brain Res* 928: 40–49, 2002.
53. Sobey CG, Heistad DD, Faraci FM. Mechanisms of bradykinin-induced cerebral vasodilatation in rats. Evidence that reactive oxygen species activate K+ channels. *Stroke* 28: 2290–2294, 1997; discussion 2295.
54. Song D, Yao R, Pang CC. Altered vasodilator role of nitric oxide synthase in the pancreas, heart and brain of rats with spontaneous type 2 diabetes. *Eur J Pharmacol* 591: 177–181, 2008.
55. Stepp DW, Pollock DM, Frisbee JC. Low-flow vascular remodeling in the metabolic syndrome X. *Am J Physiol Heart Circ Physiol* 286: H964–H970, 2004.
56. Tanne D, Koren-Morag N, Goldbourt U. Fasting plasma glucose and risk of incident ischemic stroke or transient ischemic attacks: a prospective cohort study. *Stroke* 35: 2351–2355, 2004.
57. Vermeer SE, Sandee W, Algra A, Koudstaal PJ, Kappelle LJ, Dippel DW. Impaired glucose tolerance increases stroke risk in nondiabetic patients with transient ischemic attack or minor ischemic stroke. *Stroke* 37: 1413–1417, 2006.
58. Wei EP, Kontos HA, Patterson JL Jr. Dependence of pial arteriolar response to hypercapnia on vessel size. *Am J Physiol* 238: 697–703, 1980.
59. Xiang L, Dearman J, Abram SR, Carter C, Hester RL. Insulin resistance and impaired functional vasodilation in obese Zucker rats. *Am J Physiol Heart Circ Physiol* 294: H1658–H1666, 2008.
60. Yang ST, Chang HH. Nitric oxide of neuronal origin mediates NMDA-induced cerebral hyperemia in rats. *NeuroReport* 9: 415–418, 1998.
61. Yang ST, Mayhan WG, Faraci FM, Heistad DD. Mechanisms of impaired endothelium-dependent cerebral vasodilatation in response to bradykinin in hypertensive rats. *Stroke* 22: 1177–1182, 1991.